THE ROLE OF SIMULATED SMALL-SCALE OCEAN VARIABILITY IN INVERSE COMPUTATIONS FOR OCEAN ACOUSTIC TOMOGRAPHY

Brian Dushaw[a], Hanne Sagen[a]

[a]Nansen Environmental and Remote Sensing Center, Thormøhlens gate 47, 5006 Bergen, NORWAY

Brian Dushaw, Nansen Environmental and Remote Sensing Center, Thormøhlens gate 47, 5006 Bergen, NORWAY fax: (+47) 55 20 58 01, e-mail: brian.dushaw@nersc.no

Abstract: *Ocean acoustic tomography depends on a suitable reference ocean environment with which to set the basic parameters of the inverse problem. Some inverse problems may require a reference ocean that includes the small-scale variations from internal waves, small mesoscale, or spice. Tomographic inversions that employ data of stable shadow zone arrivals, such as those that have been observed in the North Pacific and Canary Basin, are an example. Estimating temperature from the unique acoustic data that have been obtained in Fram Strait is another example. The addition of small-scale variability to augment a smoothed reference ocean is essential to understanding the acoustic forward problem in these cases. Rather than a hindrance, the stochastic influences of the small scale can be exploited to obtain accurate inverse estimates. Inverse solutions are readily obtained, and they give computed arrival patterns that matched the observations. The approach is not ad hoc, but universal, and it has allowed inverse estimates for ocean temperature variations in Fram Strait to be readily computed on the several acoustic paths for which tomographic data were obtained.*

Keywords: *acoustic tomography, acoustic scattering, inverse techniques, Fram Strait, Canary Basin*

1. INTRODUCTION

Ocean acoustic tomography consists of four basic steps [1]. First, the signals from acoustic propagation over some distance through the ocean are recorded. Second, the equivalent acoustic propagation is computed using a ***reference ocean***, or a suitably realistic representation for the acoustic environment. This computation is the ***acoustic forward problem***, which is an analysis to understand the essential factors governing the acoustic propagation and a computation of an acoustic arrival pattern that matches the recorded arrival patterns reasonably well. The discrepancies between the computed and measured arrival patterns indicate the essential information provided by tomography. Third, a representation of the ocean variability is constructed such that the variability can be modeled by a set of parameters, and the inverse components and inverse itself are computed. Lastly, the inverse solution is tested by computing acoustic propagation through the "corrected" acoustic environment to verify that the new, computed arrival pattern agrees with that recorded. Analyses of the model variances and inverse uncertainties are required and integral aspects of the inverse problem. The inverse solution then passes to the realm of physical oceanography for further analysis.

The reference ocean employed for the forward problem is most often a smooth climatology such as the World Ocean Atlas, a smoothed hydrographic section [2], or an ocean model or state estimate [3]. There are several examples of instances where the effects of small-scale variability (internal waves, spice variations, small mesoscale) are essential to understanding the forward problem, however [4; 5; 6; 7]. The influences of small-scale variablity on long-range acoustic propagation were perhaps first highlighted with the observations of the SLICE'89 experiment at 1-Mm range in the central North Pacific [8]. Shadow-zone arrivals, which are stable, ray-like arrivals that occur at times and depths outside the arrival pattern predicted using a smooth sound speed section [3; 5; 7; 9], are an obvous example of the influence of small-scale variability. How can such data be exploited for ocean estimation by an inverse when they cannot be represented by a conventional forward problem? The addition of simulated, yet realistic, small-scale variablity to a forward-problem environment can be essential to computing an inverse estimate. This paper summarizes the discussions of this problem published by Dushaw and Sagen 2017 [10].

2. CASE 1: DEEP, SHADOW-ZONE ARRIVALS

Deep, shadow-zone arrivals give stable time series of travel times that are readily identified with extensions of branches of a time front computed from a smoothed ocean realization [3; 5; 7; 9]. Indeed, shadow-zone arrivals were a significant fraction of data obtained during the decade-long (1996–2006) Acoustic Thermometry of Ocean Climate (ATOC) project. They represent valuable data, but a ray path associated with them cannot be computed using a smooth reference ocean. An inverse employing these data with such a reference ocean is therefore technically not possible. Such arrivals can be computed, and a ray path determined for them, by augmenting a smooth reference ocean with small-scale variability [5]. These arrivals have been referred to as "nongeometric," perhaps as a result of the notion that they arose from diffraction, but that word is incorrect. They can be

identified with geometric rays computed using a more complete, or realistic, reference ocean.

The nature of shadow-zone arrivals can be illustrated using a notional 2000-km long acoustic path along 25°N in the North Pacific. A good representation for the sound speed section can be computed from the 2009 World Ocean Atlas (WOA09). The internal wave

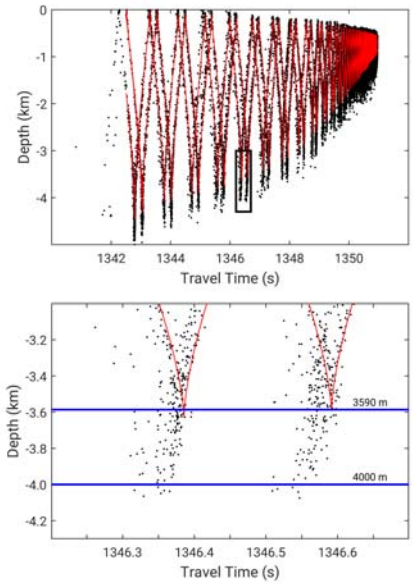

Fig. 1: Time fronts computed for a 2000-km zonal section in the midlatitude North Pacific. The red pattern indicates the time front computed from the 2009 World Ocean Atlas, while the black dots indicate the same time front that includes the effects of internal waves. The density of dots corresponds to acoustic intensity. The lower panel indicates a close up of the figure above for the box indicated. A receiver at 4-km depth would detect stable ray arrivals, although the predicted arrivals from the smooth climatology lie about 410 m above this depth.

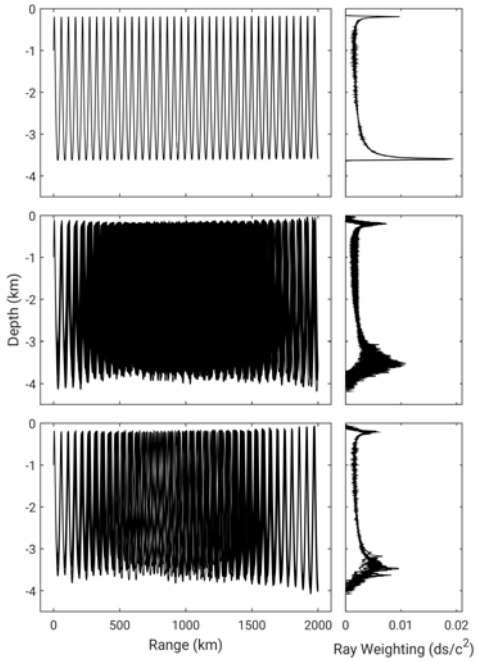

Fig. 2: Rays associated with the arrival cusp at about 1346.6-s travel time of the time-fronts of Fig. 1. Top: the ray through the smooth climatology to the cusp depth at 3590 m. Middle: under the influence of internal wave fluctuations, the same ray becomes

many rays and the ray turning depths become irregular. Bottom: the ray paths through a fluctuating ocean to a receiver at 4-km depth. The right-most panels indicate the path sampling with depth of the rays. The sampling of the shadow zone ray is similar to that of the direct arrival at the time front cusp 410 m above when scintillations are present.

model of Colosi and Brown [2] can be used to approximate the effects of internal waves on acoustic propagation. Time fronts computed for such an acoustic path, with and without the effects of internal waves, are shown in Fig. 1. The characteristic extensions of the lower cusps, or caustics, of the time front as a consequence of internal wave scattering are evident; this extension can be several hundred meters [5; 9] (Fig. 1). A receiver at 4000-m depth, for example, would detect several more ray arrivals than could be predicted using just the smooth climatology.

For any point on the time front, the computed arrival pulse is obviously no longer a single ray arrival, but it has a width of perhaps 50 ms. The specific rays associated with the predicted arrivals give the spatial sampling for the inverse problem. Three sets of rays from the lower panel of Fig. 1 may be of interest (Fig. 2). For the smooth ocean reference ocean, only 4 eigenrays were obtained to a notional receiver at the maximum depth of the time front cusp at 3590 m. For the same reference and receiver depth, but including internal wave variations, 210 rays were obtained. The cusp of the time front is a caustic which corresponds to a high ray density, or equivalently, a high acoustic amplitude. One effect of the internal wave variations is that the high-amplitude reception becomes split into many ray paths with varying lower and upper turning depths. Lastly, at a depth of 4000 m, or 410 m below the cusp of the smooth-ocean time front, 10 rays are obtained, with similar variations in turning depth.

One way to assess the impact of small-scale fluctuations on the ray paths, hence the inverse, is to compute the ray weighting as a function of depth. The small internal-wave scales included in the reference ocean have horizontal scales of O(100–1000) m, while the perturbative sound speed that is of oceanographic interest has horizontal scales of O(10–1000) km. The ray weighting quantifies the impact particular travel times can have on the inverse solution. The ray kernel for the rays of Fig. 2 are shown in the right hand panels. In this case, the kernel has been summed horizontally, giving the weighting as a function of depth. In the top-most panel, the ray from the smoothed reference ocean gives ray weighting with sharp increases in value at the ray turning depths. The aspect ratio of the ray figures can be misleading; most of the ray arc length occurs at the ray turning depths. One effect of the small-scale variability is to induce variations in the upper and lower turning depths of the rays. As a consequence of the irregular turning depths, the ray weighting is blunted and broadened in depth. The ray kernels for the rays to receivers at 3590 or 4000 m depths, are similar, though there are many more rays to the shallower depth where the acoustic intensity is greater.

3. CASE 2: SPICE-SCATTERED ARRIVALS

"Shadow-zone arrivals" are not limited to the lower (or upper) cusps of the timefront. The ray arrivals recorded in the Canary Basin during 1997-8 for the purpose of measuring the properties of Meddies included a clear, unpredicted arrival at the end of the arrival pattern (Fig. 3) [7]. This arrival was recorded by a receiver near the sound channel axis. It arose from the extension of a branch of the timefront to later times as a result of scattering from small-scale variations of spice. Such variations are ubiquitous along the sound channel axis in this region. Its existence is entirely a consequence of such scattering, and

any inverse employing this arrival would necessarily require a reference ocean incorporating small-scale variability.

4. CASE 3: ACOUSTIC PROPAGATION IN FRAM STRAIT

The extraordinary small-scale variability of Fram Strait has made it challenging to understand the regional oceanography by hydrographic sections or moorings. A pilot

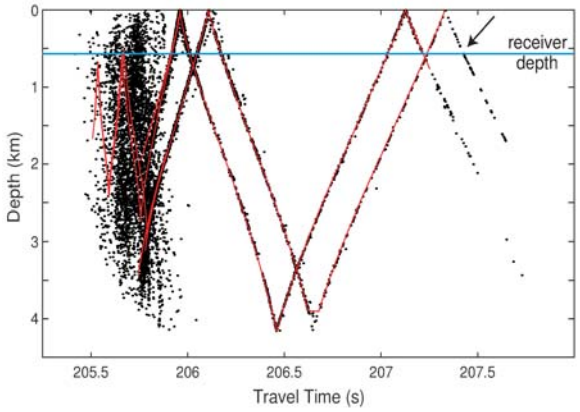

Fig. 3: Time fronts computed for 309-km range in the Canary Basin from the smooth 2009 World Ocean Atlas (red) and from the World Ocean Atlas including internal wave and small-scale spice variability (black dots). An experiment conducted in 1997 with a receiver at 600-m depth recorded a stable ray reception corresponding to the arrival indicated by the arrow [7]. This arrival is a product of small-scale acoustic scattering.

tomography measurement in 2008–2009, the "Developing Arctic Modelling and Observing Capabilities for Long-term Studies" (DAMOCLES) program, was described by Sagen, et al. [11], while the subsequent "Acoustic Technology for Observing the Interior of the Arctic Ocean" (ACOBAR) progam (2011–2012) was described by Sagen, et al. [2]. The small-scale variablity has a large impact on the acoustic propagation in the region. Sagen, et al. [2] examined the acoustic predictability of the ACOBAR data by employing smoothed hydrographic sections and comparing acoustic predictions to suitably filtered observations. They sought a deterministic solution to the ray sampling problem, requiring a suppression of small-scale effects by filtering methods. With the unique stratification in Fram Strait, the precise acoustic propagation is dependent on the mesoscale state, which is constantly changing [2; 6]. Acoustic predictions using a smoothed climatology or hydrographic section give only a small set of rays, but a typical arrival pattern for the region consists of a single, broad arrival of perhaps 100 ms width, sometimes together with a few distinct pulses from bottom-reflected rays. With a Rossby radius of deformation of 4–6 km, the small mesoscale variablity of the region is essential to understanding the nature of the acoustic propagation [6]. The contributions from internal-wave variability are minor, as a consequence of the stratification in this region.

Inverse estimates from DAMOCLES and ACOBAR data were obtained by employing a reference ocean formed by the World Ocean Atlas as the background sound speed plus sound speed variations caused by small mesoscale variability (Fig. 4). When realizations for small mesoscale variations were added to the World Ocean Atlas, many more rays were obtained and the predicted patterns were similar to observations, both DAMOCLES [6] and ACOBAR. In this case, rather than just a few rays, several hundred rays were

obtained. Despite the large number of rays, their spatial sampling was similar, normally cycling between the ocean's surface and 1000–1500-m depths.

This approach to the inverse of tomography data obtained in Fram Strait has worked well, providing estimates of range- and depth-averaged temperature along DAMOCLES and ACOBAR acoustic paths with little trouble. The inverse solutions were found to give acoustic arrival patterns in agreement with the data (Fig. 5). The entirely fictional small mesoscale environment employed with the reference ocean does not affect the temperature estimates consequentially (Fig. 6). It merely lends an essential stochastic nature to the acoustic propagation.

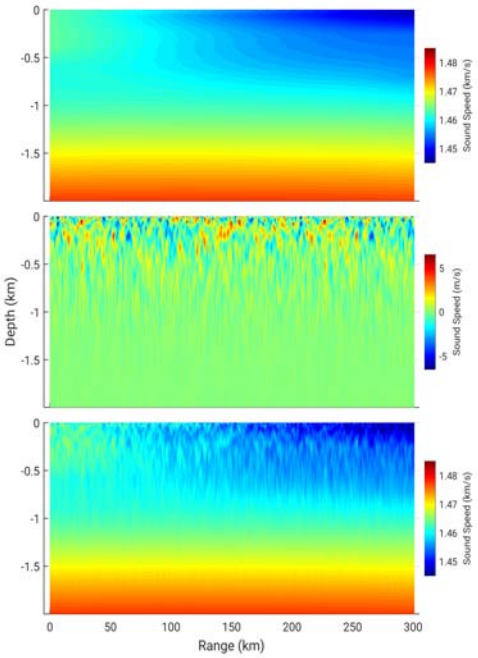

Fig. 4: (bottom) The reference sound speed section for computing inversions of Fram Strait tomography data obtained along the ACOBAR A to B path [See 2]. Greenland is to the right, Svalbard to the left. The reference consists of the sum of (top) the 2009 World Ocean Atlas sound speed and (middle) a simulation of small mesoscale variability [6].

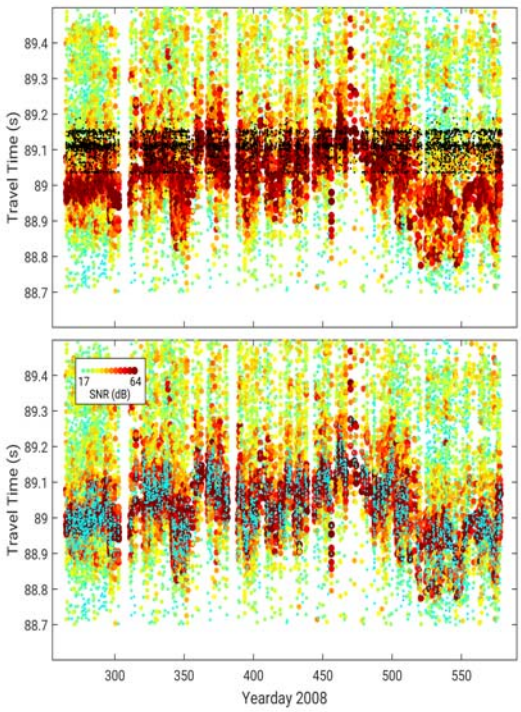

Fig. 5: Time series of acoustic travel times and amplitudes obtained by the DAMOCLES project in 2008–2009 on one of four hydrophones. The top panel shows the reference ocean travel times as the black dots, while the bottom panel shows the travel times computed using the inverse solution as the cyan dots. Comparisons to data from three other hydrophones were similar. Small-scale fluctuations give reference-ocean travel times that more closely resemble the data.

5. DISCUSSION

The approach of combining small-scale sound speed variations with a smooth ocean representation to form a reference ocean for an inverse should not be surprising. Such small-scale variations can be essential to understanding the acoustic propagation. Small-scale variations can be by internal waves, by spice, or by small mesoscale features in high latitudes. In addition, the recorded arrival patterns may depend critically on the influences of the small scale, either pulse width or entire branches of a time front. No inverse can resolve these small scales, of course, so we are dependent on using simplified statistical models.

Adding small-scale variations to a reference ocean might be considered another technique or trick that can be employed for better inverse estimates. One example of such a trick is the use of a time-dependent reference ocean that may account for a sizeable annual cycle. Accounting for the major part of the annual cycle in the reference ocean makes the inverse more linear (smaller perturbations from the reference), while at the same time prior variances are less giving smaller formal uncertainty estimates. Adding small-scale contributions to the reference ocean is a not-dissimilar trick. Such contributions should have negligible influence on the oceanographic quantitity estimated by the inverse, since the latter are large scale.

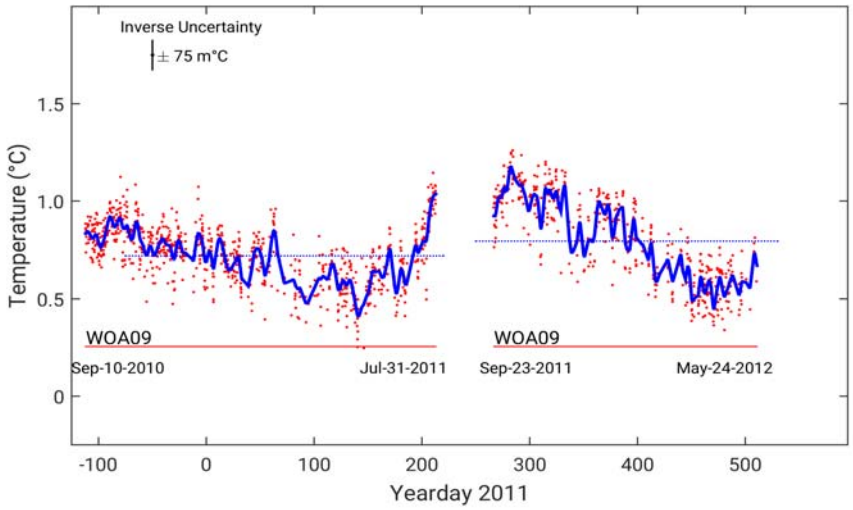

Fig. 6: Range- and depth-averaged temperature along a 301-km ACOBAR path between moorings A and B [See 2]. Depth average is over the depth interval 0 to 1000 m, which is the dominant sampling interval of the ray paths. Individual estimates are denoted by the red dots, while the blue line is a weighted cubic spline fit to those estimates. The formal inverse uncertainty for this average is about 75 m◦C, as indicated. Dates at the start and end of each time series are indicated, while the red lines indicate the equivalent average in the WOA09.

6. ACKNOWLEDGEMENTS

The ACOBAR project was funded under the 7th EU Framework Programme (Grant No. 212887). Analysis of the ACOBAR data has been carried out under funding from the Research Council of Norway through the ACOBAR II (Grant No. 226997) and UNDERICE (Grant No. 226373) projects. ENGIE E&P Norway provided additional support. The U.S. Office of Naval Research provided partial support for this work by ONR Grant N00014-10-1-0990 to the Scripps Institution of Oceanography. B.D.D. was supported by ONR Grant N00014-15-1-2186. Any opinions, findings, and conclusions or recommendations expressed in this publication are those of the authors and do not necessarily reflect the views of the Office of Naval Research.

REFERENCES

[1] **Munk, W., P. Worcester, and C. Wunsch,** *Ocean Acoustic Tomography,* Cambridge, UK*:* Cambridge University Press, 456 pp., 1995.

[2] **Sagen, H., P. F. Worcester, M. A. Dzieciuch, F. Geyer, S. Sandven, M. Babiker, A. Beszczynska-Möller, B. D. Dushaw, and B. Cornuelle,** Resolution, identification, and stability of broadband acoustic arrivals in Fram Strait, *J. Acous. Soc. Am.*, 141, 2055–2068, doi: 10.1121/1.4978780, 2017.

[3] **Dushaw, B. D., P. F. Worcester, W. H. Munk, R. C. Spindel, J. A. Mercer, B. Howe, K. Metzger, Jr., T. G. Birdsall, R. K. Andrew, M. A. Dzieciuch, B. D. Cornuelle, and D. Menemenlis**, A decade of acoustic thermometry in the North Pacific Ocean, *J. Geophys. Res.*, 114, C07021, doi: 10.1029/2008JC005124, 2009.

[4] **Colosi, J.**, *Sound Propagation through the Stochastic Ocean*, Cambridge, UK: Cambridge University Press, 424 pp., 2016.

[5] **Van Uffelen, L. J., P. F. Worcester, M. A. Dzieciuch, D. L. Rudnick, and J. A. Colosi,** Effects of upper ocean sound-speed structure on deep acoustic shadow-zone arrivals at 500- and 1000-km range. *J. Acous. Soc. Am.*, 127, 2169–2181, doi:10.1121/1.3292948, 2010.

[6] **Dushaw, B. D., H. Sagen, and A. Beszczynska-Möller,** On the effects of small-scale variablity on acoustic propagation in Fram Strait: The tomography forward problem, *J. Acoust. Soc. Am.*, 140, 1286–1299, doi: 10.1121/1.4961207, 2016.

[7] **Dushaw, B. D., F. Gaillard, and T. Terre**, Acoustic tomography in the Canary Basin: Meddies and tides, *J. Geophys. Res.*, submitted, 2017.

[8] **Duda, T. F., S. M. Flatté, J. A. Colosi, B. D. Cornuelle, J. A. Hildebrand, W. S. Hodgkiss, P. F. Worcester, B. M. Howe, J. A. Mercer, and R. C. Spindel**, Measured wave-front fluctuations in 1000-km pulse propagation in the Pacific Ocean, *J. Acoust. Soc. Am.*, 92, 939–955, doi: 10.1121/1.403964, 1992.

[9] **Dushaw, B. D., B. M. Howe, J. A. Mercer, R. C. Spindel, A. B. Baggeroer, D. Menemenlis, C. Wunsch, T. G. Birdsall, C. Clark, J. A. Colosi, B. D. Cornuelle, M. Dzieciuch, and W. Munk**, Multimegameter-range acoustic data obtained by bottom-mounted hydrophone arrays for measurement of ocean temperature, *IEEE J. Ocean. Engin.*, 24, 202–214, doi: 10.1109/48.757271, 1999.

[10] **Dushaw, B. D., and H. Sagen**, The role of small-scale ocean variability in inverse computations for ocean acoustic tomography, *J. Acous. Soc. Am.*, submitted, 2017.

[11] **Sagen, H., B. D. Dushaw, E. K. Skarsoulis, D. Dumont, M. Dzieciuch, and A. Beszczynska-Möller**, Time series of temperature in Fram Strait determined from the 2008–9 DAMOCLES acoustic tomography measurements and an ocean model, *J.*